Materials Science and Engineering A 492 (2008) 481–485

Contents lists available at ScienceDirect

Materials Science and Engineering A

journal homepage: www.elsevier.com/locate/msea

Hot deformation behavior of SiCp/AZ91 magnesium matrix composite fabricated by stir casting

X.J. Wang*, X.S. Hu, K. Wu, K.K. Deng, W.M. Gan, C.Y. Wang, M.Y. Zheng

School of Materials Science and Engineering, Harbin Institute of Technology, Harbin 150001, PR China

ARTICLE INFO

Article history:
Received 3 November 2007
Received in revised form 1 April 2008
Accepted 22 May 2008

Keywords:
Magnesium matrix composite
Stir casting
Compression
Activation energy
SiC

ABSTRACT

The uniaxial compressive deformation behavior of a 10 vol.% SiC particulate reinforced AZ91 magnesium matrix composite (SiCp/AZ91) fabricated by stir casting is investigated at elevated temperature (250–400 °C). Peak stresses and flow stresses decrease as temperatures increase and strain rates decrease. The extent of dynamic recrystallization (DRX) becomes less as temperatures decrease at 250–350 °C or strain rates increase, and recrystallization occurs mainly within the intergranular regions rich of particles. Dynamic recrystallization accomplishes at 400 °C even at the strain rate of 1 s^{-1}. An analysis of the effective stress dependence on strain rate and temperature gives a stress exponent of $n = 5$ and a true activation energy of $Q = 99$ kJ/kJ. The value of Q is close to the value for grain boundary diffusion in Mg. It is concluded that the deformation mechanism of SiCp/AZ91 composite during hot compression is controlled by the dislocation climb.

1. Introduction

Magnesium matrix composites overcome the demerits of the monolithic magnesium alloys, such as low stiffness, elastic modulus and strength [1]. What is more, particulate reinforced magnesium matrix composites fabricated by stir casting are very cost-effective, promising a widespread application to aerospace, defense and automobile industries [1,2]. In order to exploit the benefits of magnesium matrix composites, it is important to develop secondary processing which can effectively produce complex engineering components directly from wrought products [3]. But few works are conducted on studying the hot deformation behavior of particulate reinforced magnesium matrix composites [2].

For the industrial applications, the flow stress is the most important property of the material during processing. The power-law Eq. (1) has been extensively applied to represent the relationship between flow stress and strain rate [3–9]:

$$\dot{\varepsilon} = A\left(\frac{b}{d}\right)^{q}\left(\frac{\sigma}{G}\right)^{n}\exp\left(-\frac{Q_a}{RT}\right) \tag{1}$$

where A is a constant, n the stress exponent, G the shear modulus, σ flow stress, R the gas constant, Q_a the apparent activation energy, b the magnitude of the Burgers vector, d the grain size and p (=2 or 3) the grain size exponent. Theoretically, we can understand the physics of deformation by calculating the stress exponent and the activation energy. In practice, however, the stress exponent n is very high, and the values of apparent activation energy for metal matrix composite are much higher than the values of self-diffusion in their matrix alloys [4,5,10,11]. It is a standard procedure in metal matrix composites to interpret the deformation in the term of an effective stress, σ_e, which is defined as $(\sigma - \sigma_0)$ where σ_0 is a threshold stress delineating a lower limiting stress for any measurable flow [7–9]. Under these conditions, Eq. (1) is modified into:

$$\dot{\varepsilon} = A\left(\frac{b}{d}\right)^{q}\left(\frac{\sigma - \sigma_0}{G}\right)^{n}\exp\left(-\frac{Q}{RT}\right) \tag{2}$$

where Q is true activation energy, and σ_0 is estimated either by plotting against on linear axes for selected values of n and extrapolating linearly to zero strain rate or by directly extrapolating the deformation data to very low strain rates. Threshold stress and true activation energy have been extensively studied in aluminium matrix composites [4,5,11], but corresponding works on magnesium matrix composites are very few [10,12–14]. Nieh et al. [13] have studied superplasticity of SiCp/ZK60 composite and found that the superplastic deformation was one of grain boundary sliding controlled by grain boundaries diffusion mechanism. The creep of magnesium strengthened with high volume fractions of yttria dispersoids was studied by Han and Dunand [15]. They found that two separate creep regimes were observed in the composite, at low stresses, both the apparent stress exponent and the apparent activation energy are low, while at high stresses, these parameters are much higher and increase, respectively, with increasing

* Corresponding author. Tel.: +86 45186402291; fax: +86 45186413922.
E-mail address: wang81113@126.com (X.J. Wang).

0921-5093/$ – see front matter © 2008 Elsevier B.V. All rights reserved.
doi:10.1016/j.msea.2008.05.046

temperature and stress [15]. Ferkel and Mordike have investigated the creep behavior of magnesium strengthened by SiC nanoparticles [16]. Some researchers have studied the deformation behavior of alloy system reinforced with intermetallic particles, for example Mg–Zn–Y [17,18] and Mg–Si alloys [19].

In this paper, the deformation behavior of SiCp/AZ91 is investigated at elevated temperature (250–400 °C), and the stress exponent and true activation energy are calculated using Eq. (2).

2. Experimental procedure

The 10 vol.% SiCp/AZ91 composite used in this work is fabricated by stir casting. The average diameter of SiCp is about 10 μm. The details for stir casting processing have been described in references [20]. The particle distribution is uniform at macroscopical scale, but particles are segregated at a microscopical scale near grain boundary regions, which is a typical "necklace-type" particle distribution in metal matrix composites fabricated by stir casting [20]. Cylindrical billets of 8 mm diameter and 12 mm height are machined from the composite. Before compression test, specimens were subjected to T4 treatment (380 °C, 2 h + 415 °C, 24 h) in order to eliminate the influence of second phase $Mg_{17}Al_{12}$. The average grain size of the composite (T4) is about 95 μm. The Compressive tests are conducted using a compute-controlled Gleeble-1500D test machine within a temperature range between 250 and 400 °C and a strain rate range between 0.001 and 1 s^{-1} in a vacuum. Graphite lubricant was used for the compression tests in order to reduce friction. The specimens are held for 5 min after the specimen temperature reached the given temperature, and the tests start.

3. Results and discussion

3.1. True stress–strain curves and microstructure

The flow stresses and peak stresses increase with decreasing temperatures or with increasing strain rates, as shown in Figs. 1 and 2. All the true stress–strain curves show an initial work hardening period followed by a regime of near steady-state flow, which results from hardening and softening of the composite during hot deformation. At the primary stage of hot compression, generation and pile-up of the dislocation lead to work hardening. Subsequently, the rate of hardening is balanced by the rate of softening due to dynamic recrystallization (DRX) [6]. The strains corresponding to the peak stresses decrease as temperatures increase and strain rates decrease, because greater amount of deformation is needed to form a recrystallization nucleus at higher strain rates and lower temperatures.

The typical microstructure of SiCp/AZ91 composite hot compressed is shown in Fig. 3. The extent of DRX becomes less as strain rates increase at 250–350 °C and temperatures decrease. DRX accomplishes at 400 °C even at the strain rate of 1 s^{-1}. So DRX is easy to occur at high temperatures and lower strain rates, which results in early arrival of peak stresses and softening in the strain–stress curves, as shown in Figs. 1 and 2. Recrystallized regions are mainly located in the intergranular regions where particle segregates, and recrystallization do not occur in the intragranular regions which are poor of particles, as shown in Fig. 3(a)–(c) and Fig. 4(a)–(c). This indicates that particles stimulate DRX [2]. As recrystallization progresses (in Figs. 3 and 4), recrystallized regions extend from the intergranular regions to the central regions of grains. It is very similar to rotational DRX observed in Mg alloy [21,22]. For rotational DRX model, fine DRX grains are formed at the distortion region in the vicinity of grain boundaries [22]. Especially at high temperature, slip in non-basal systems may operate, thus giving rise to rotated regions and accommodating the imposed external deformation [22]. As strain increases further, subgrains form in these mantle regions by dynamic recovery and ultimately high angle boundaries appear by subboundary migration and coalescence [22]. In the composite under study, the presence of SiCp leads to inhomogeneous deformation [23]. The dislocation structures resulting from this inhomogeneous deformation give rise to the formation of locally rotated regions to material adjacent to SiCp, which is called particle deformation zones (PDZ) [23]. PDZ are ideal sites for the development of recrystallization nucleus because of high dislocation density and large orientation gradient in PDZ [23]. SiCp are segregated at grain boundaries in this composite, which is a typical "necklace-type" particle distribution. So, DRX grains are also formed in the vicinity of grain boundaries in this composite. This is very similar to the rotational DRX model.

3.2. The activation energy for plastic deformation

The true stresses at $\varepsilon = 0.2$ are selected to calculate the activation energy. A plot of σ against $\dot{\varepsilon}^{1/n}$ ($n = 2, 3, 5, 8$) is adopted to determine the threshold stress, as shown in Fig. 5. $n = 5$ and $n = 8$ give the best linear fit among the assumed stress exponent "n". The calculated threshold stresses are minus using $n = 8$, so we discard the value. As shown in Fig. 6, the threshold stresses are calculated using $n = 5$ to be 44, 29, 12 and 10 MPa at 250, 300, 350 and 400 °C, respectively. Calculations give the stress exponent of $n = 5$, which indicates that the hot deformation is controlled by the climb of dislocations [10], and true activation energy of $Q = 99$ kJ/mol, as shown in Fig. 6(b) and (c). The value of Q is very close to the value for grain boundary diffusion (92 kJ/mol) [24]. Li et al. investigated the high-temperature compressive behavior of SiC whisker reinforced AZ91 composite and obtained that n increases from 5.2 to 8.3 with temperature decreasing from 400 to 200 °C, and that the apparent activation energy was much higher than the value of Mg self-diffusion [14]. Their high values of n and Q_a may be due to the high volume fraction of SiC whiskers [4].

The analyses of deformation data for unreinforced materials, it is usual to anticipate that the value of n will take values of 3, 5 or 8, representing the viscous glide of dislocation, climb of dislocation, or a constant substructure model in which the microstructure remain constant during deformation, respectively [4,11]. For $n = 5$ or 8, the anticipated activation energy is close to the value for self-diffusion in the crystallization in aluminium-based materials [4,24], but the calculated activation energy in our study is close to the value for grain boundary diffusion in Mg when the stress exponent n is equal to 5. Springarn and Nix [25] have established a creep model based on the climb of dislocations at grain boundaries. In the creep model [25], n varies 1–5, and the activation energy corresponds to grain boundary diffusion. So our calculated results are supported by their theory. Han and Dunand [15] also found $n = 5$ in high-stress regime in magnesium strengthened with high volume fractions of yttria dispersoids, which confirms our results. Very limited information is presently available on the hot deformation of composite fabricated with an AZ91 matrix alloy, but more information is available on Mg alloys [12]. **Vagarali and Langdon have also found that creep in polycrystalline Mg occurs with an activation energy close to the value for grain boundary diffusion and with a stress exponent of 5 at temperatures below 350 °C, which is very consistent with our results [24]. Somekawa et al. [9] have also found that creep mechanism of AZ91 alloy is dislocation-climb-controlled in the deformation conditions which are similar to compression condition in our study. Our results agree with the deformation mechanism maps for Mg alloys drawn by Somekawa et al. [9]. So all of these confirm the hot deformation mechanism of SiCp/AZ91 composite

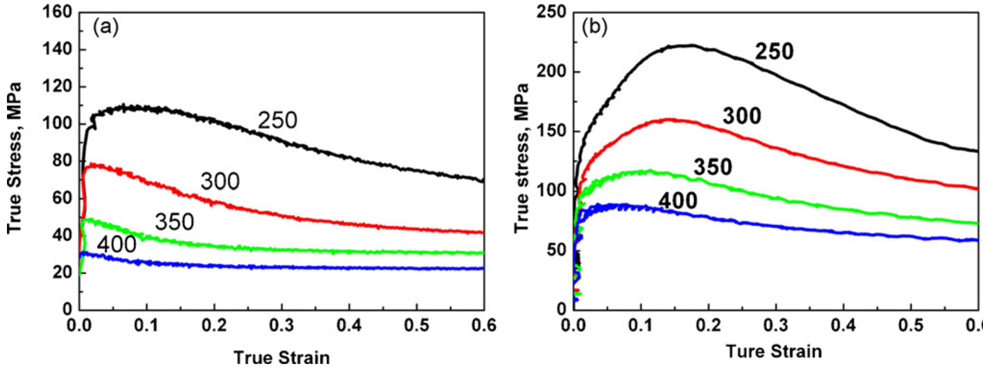

Fig. 1. Typical true stress–strain curves of SiCp/AZ91 composite hot compressed at different temperatures (250–400 °C), and strain rate of (a) 0.001 and (b) 1 s^{-1}.

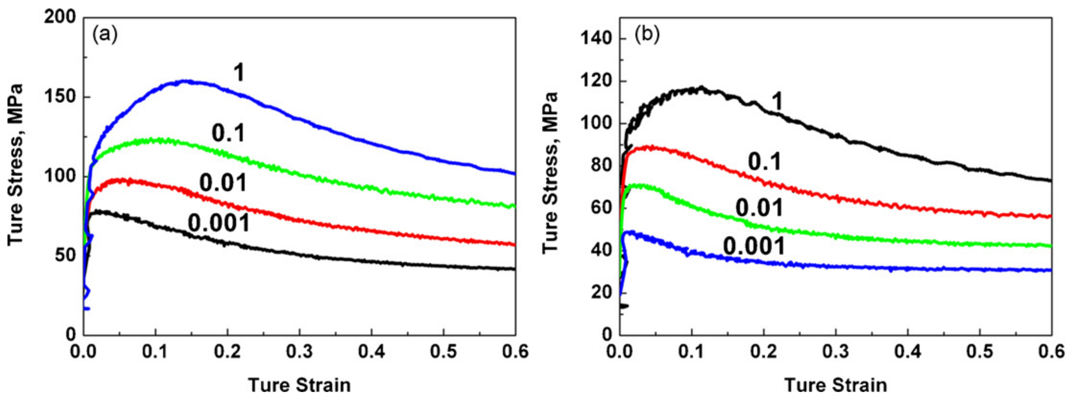

Fig. 2. Typical true stress–strain curves of SiCp/AZ91 composite hot compressed at different strain rate, and temperature of (a) 300 and (b) 350 °C.

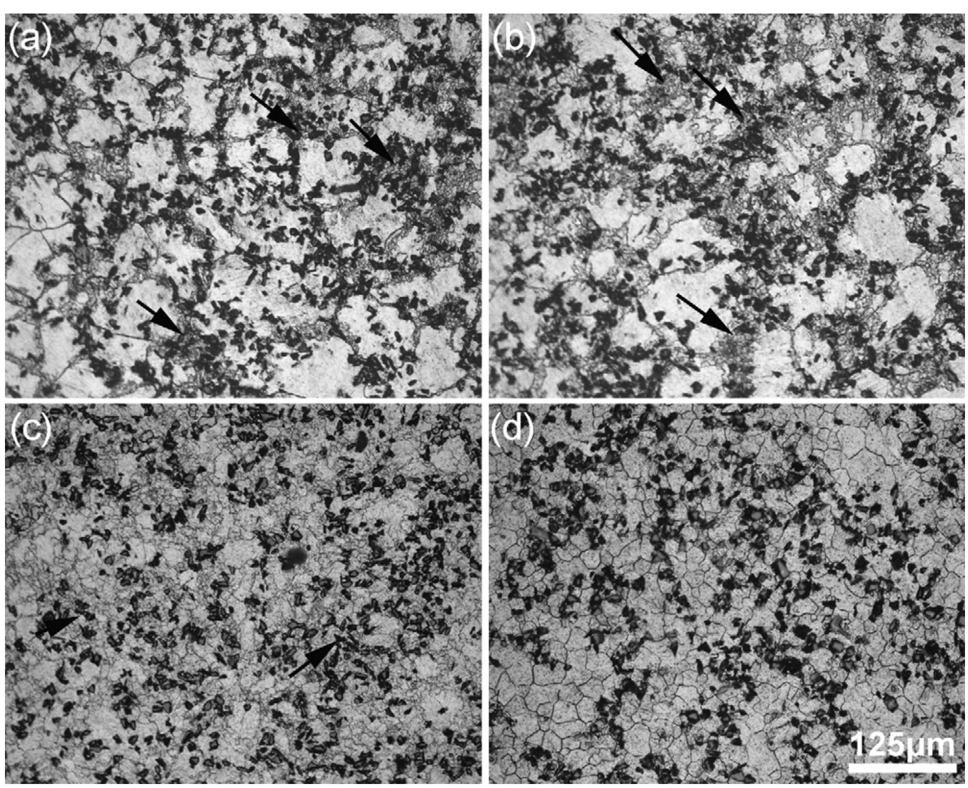

Fig. 3. Optical microstructure of SiCp/AZ91composite hot compressed at different parameters (arrows represent DRX regions): (a) 300 °C, 0.01 s^{-1}; (b) 300 °C, 0.001 s^{-1}; (c) 350 °C, 0.01 s^{-1}; (d) 400 °C, 0.01 s^{-1}.

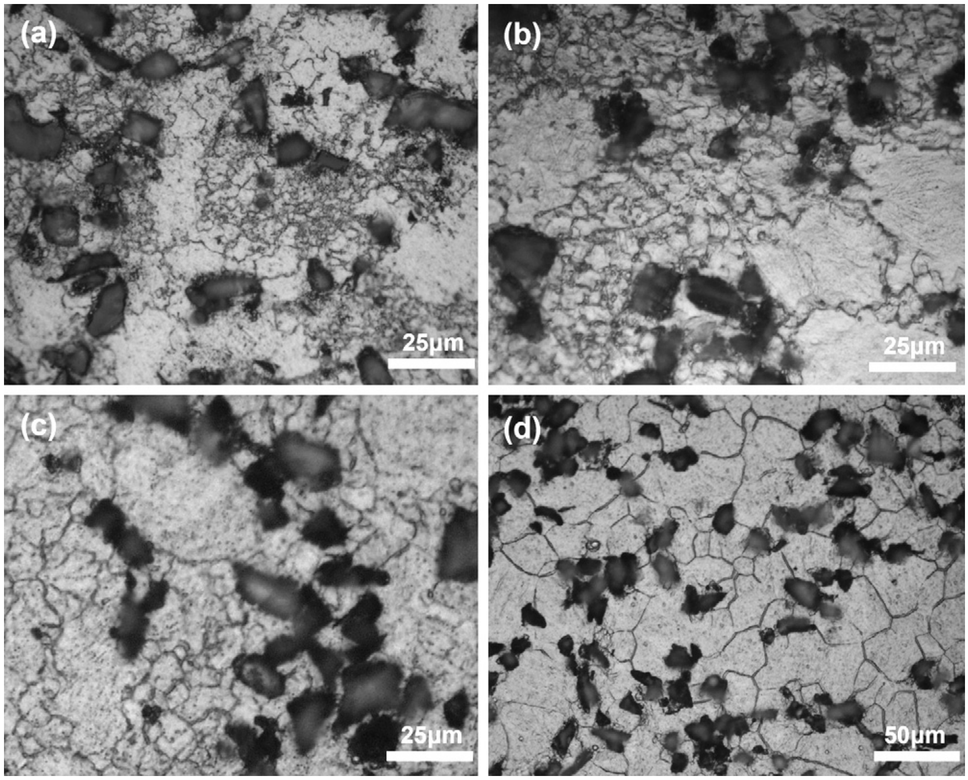

Fig. 4. Further magnification of Fig. 3(a)–(d), respectively.

is controlled by dislocation climb. The particle distribution characteristics of the composite under study may influence the physics of the deformation. As shown in Figs. 3 and 4, most of particles segregate in the intergranular regions [1,15]. So there are many particle/matrix interfaces and high dense dislocations in the intergranular regions, which makes grain boundary diffusion easy to occur during hot deformation. As shown in Figs. 3 and 4, DRX occurs mainly in the intergranular regions, which may support that grain boundary diffusion plays a predominant role during hot deformation.

In our study, the threshold stresses decrease from 44 to 10 MPa as temperature increase from 250 to 400 °C. Watanabe investigated the superplasticity of the AZ31, and calculated the threshold stress to be 5.2, 2.8, 2.4 and 1.6 MPa at 225, 350, 375 and 400 °C, respectively [26]. And the threshold stresses in our study are also much higher than the threshold stresses for Mg–Al–Zn alloys (AZ31, AZ61, AZ91) calculated by Del Valle et al. [27]. Del Valle et al. [27] have found that the threshold stress decreases with decreasing grain size. The grain sizes of those alloys are much smaller than that of the composite under study

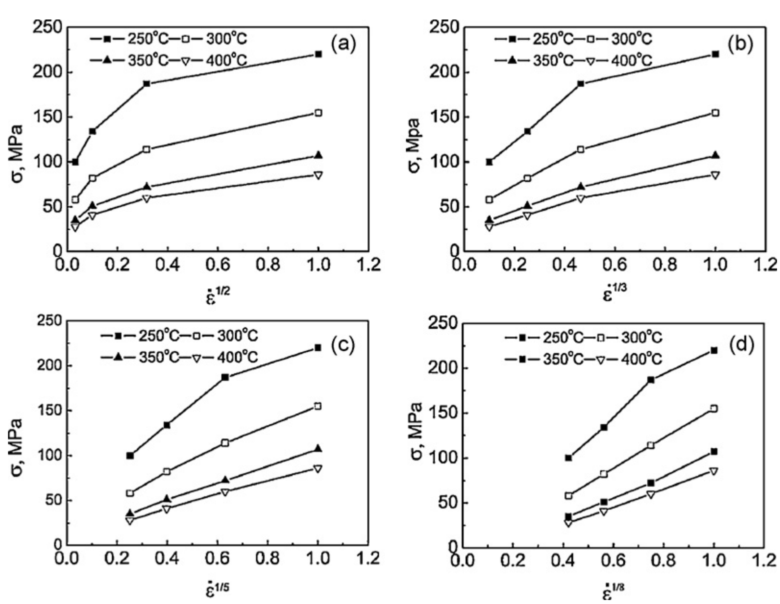

Fig. 5. The plots of flow stress vs $\dot{\varepsilon}^{1/n}$. (a) $n = 2$, (b) $n = 3$, (c) $n = 5$, (d) $n = 8$.

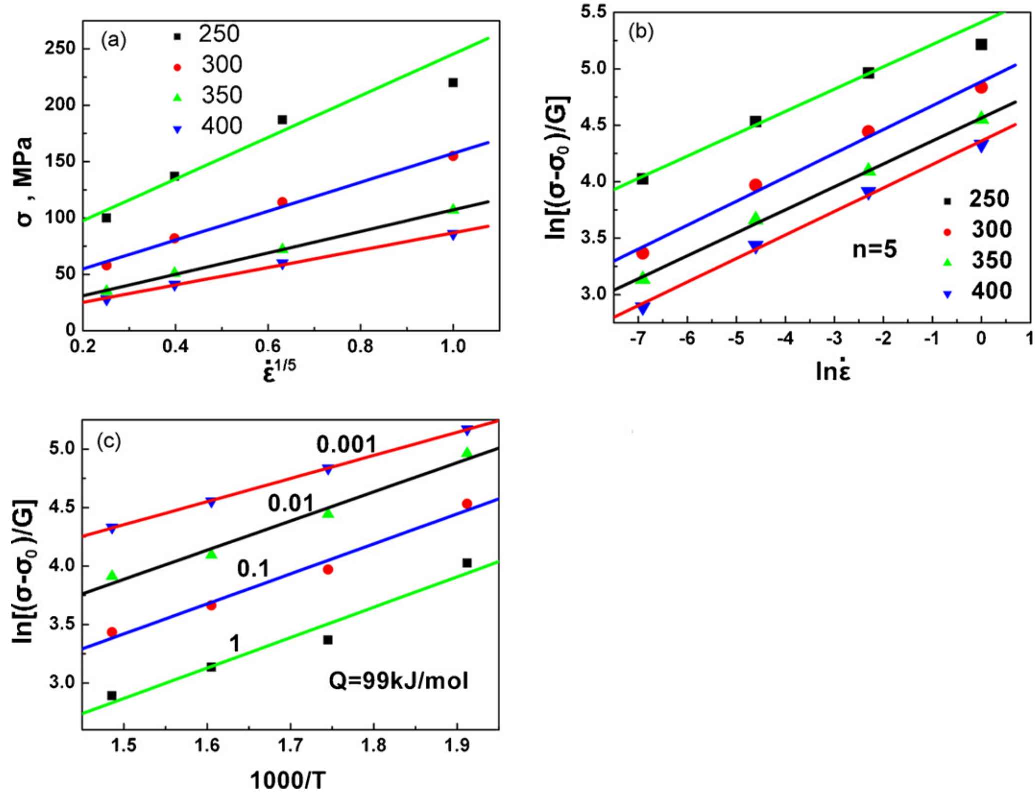

Fig. 6. The variation of (a) flow stress vs $\dot{\varepsilon}^{1/5}$, (b) $\ln[(\sigma-\sigma_0)/G]$ vs $\ln\dot{\varepsilon}$ and (c) $\ln[(\sigma-\sigma_0)/G]$ vs $1000/T$.

[26,27]. So the higher value of threshold stresses in the composite under study results from presence of SiCp and large grain size [4,10,12,27]. However, the values of threshold stress in the composite under study are much lower than the value calculated by Han and Dunand [15]. This is due to high volume fractions of ultra-fine yttria dispersoids in Han and Dunand's composite [15].

In order to account for the temperature dependence of the threshold stress τ_0 in aluminium-based materials, Mohamed et al. development a semi-empirical Arrhenius relationship of the form [4,12,28],

$$\frac{\tau_0}{G} = B\exp\left(\frac{Q_0}{RT}\right) \tag{3}$$

where B is a constant and Q_0 is an energy term which is tentatively associated with the binding energy between the dislocation and obstacles in the glide plane. Both our and Watanabe's values of the threshold stress is not fit to Eq. (3). But Han and Dunand [15] have calculated a threshold stress for Mg–yttria composite that follows an Arrhenius relationship proposed by Mohamed et al. [28]. They have gotten Q_0 = 11 kJ/mol according to Eq. (3) [15].

4. Conclusion

The hot deformation of a SiCp/AZ91 composite fabricated by stir casting is investigated by compression tests. Following the standard procedure for hot deformation, the flow stressed are related to strain rat and to temperatures by means of a modified power-law equation. Calculations give n = 5 and Q = 99 kJ/mol. According to the calculated results and the published results, it is concluded that the mechanism controlling hot deformation is the climb of dislocations.

References

[1] A. Luo, Can. Metall. Q 35 (1996) 375–383.
[2] B. Inem, Mater. Sci. Eng. A 197 (1995) 91–95.
[3] M.R. Barnett, J. Light Met. 1 (2001) 167–177.
[4] Z.Y. Ma, S.C. Tjong, Compos. Sci. Technol. 61 (2001) 771–786.
[5] Y. Li, T.G. Langdon, Acta Mater. 47 (1999) 3395–3403.
[6] F.C. Ma, W.J. Lu, J.N. Qin, D. Zhang, Mater. Lett. 60 (2006) 400–405.
[7] M.E. Kassner, Prog. Mater. Sci. 45 (2000) 1–102.
[8] J.A. del Valle, F. Carreño, O.A. Ruano, Scripta Mater. 57 (2007) 829–832.
[9] H. Somekawa, K. Hirai, H. Watanabe, Y. Takigawa, K. Higashi, Mater. Sci. Eng. A 407 (2005) 53–61.
[10] P. Zhang, Scripta Mater. 52 (2005) 277–282.
[11] S. Spigareli, E. Evangelista, E. Cerri, T.G. Longdon, Mater. Sci. Eng. A 319–321 (2001) 721–725.
[12] Y. Li, T.G. Longdon, Metall. Trans. A 30 (1999) 2059–2065.
[13] T.G. Nieh, A.J. Schwartz, J. Wadsworth, Mater. Sci. Eng. A 208 (1996) 30–36.
[14] S.B. Li, M.Y. Zheng, W.M. Gan, K. Wu, Mater. Sci. Forum 475–479 (2005) 893–896.
[15] B.Q. Han, D.C. Dunand, Mater. Sci. Eng. A 300 (2001) 235–244.
[16] H. Ferkel, B.L. Mordike, Mater. Sci. Eng. A 298 (2001) 193–199.
[17] D.H. Bae, S.H. Kim, D.H. Kim, W.T. Kim, Acta Mater. 50 (2002) 2343–2356.
[18] M.Y. Zheng, S.W. Xub, K. Wa, S. Kamadob, Y. Kojima, Mater. Lett. 61 (2007) 4406–4408.
[19] M. Mabuchi, K. Higashi, Philos. Mag. A 74 (1996) 887–905.
[20] X.J. Wang, K. Wu, W.X. Huang, H.F. Zhang, M.Y. Zheng, D.L. Peng, Compos. Sci. Technol. 67 (2007) 2253–2260.
[21] J.A. Del Valle, M.T. Perez-Prado, O.A. Ruano, Mater. Sci. Eng. A 355 (2003) 68–78.
[22] S.E. Ion, F.J. Homphreys, S.H. Whice, Acta Metall. 30 (1982) 1909–1919.
[23] F.J. Humphreys, P.N. Kalu, Acta Mater. 38 (1990) 917–930.
[24] S.S. Vagarali, T.G. Langdon, Acta Metall. 29 (1981) 1969–1982.
[25] J.R. Springarn, W.D. Nix, Acta Metall. 22 (1979) 171–177.
[26] H. Watanabe, H. Tsutsui, T. Mukai, M. Kohzu, S. Tanabe, K. Higashi, Int. J. Plast. 17 (2001) 389–397.
[27] J.A. del Valle, F. Carreño, O.A. Ruano, Script Mater. 57 (2007) 829–832.
[28] F.A. Mohamed, K.T. Park, E.J. Lavernia, Mater. Sci. Eng. A 150 (1992) 21–35.